Desalination and Water Treatment
www.deswater.com
doi: 10.5004/dwt.2021.27054

220 (2021) 1–13
April

Hydrodynamic study on horizontal-axis tidal current turbine with coupling motions

Gang Xu[a], Zhen Chen[a], Mingliang Hu[b], Shuqi Wang[a,c,*]

[a]*School of Naval Architecture and Ocean Engineering, Jiangsu University of Science and Technology, Zhenjiang 212003, China, emails: g.xu@just.edu.cn (S. Wang), me_xug@qq.com (G. Xu), 83889195@qq.com (Z. Chen)*
[b]*Boat R&D Center, Hubei Sanjiang Boats Science and Technology Co., Ltd., Xiaogan 432000, China*
[c]*College of Shipbuilding Engineering, Harbin Engineering University, Harbin 150001, China, email: terry.hu7@hotmail.com*

Received 16 June 2020; Accepted 21 January 2021

ABSTRACT

Hydrodynamic characteristics of floating horizontal-axis turbine are affected by the wave-induced motion response of the floating platform for the turbine system. In order to analyze this problem, the computational fluid dynamic (CFD) technique has been adopted to simulate the hydrodynamic characteristics of the turbine with rotation and yawing coupling motions in constant inflow, and study how the hydrodynamic performance of the turbine is affected by yawing frequency, yawing amplitude, and tip speed ratio. Based on the time-varying hydrodynamic curves of the turbine from the simulation data of CFD, yawing damping coefficient can be obtained by the least-square fitting. The results demonstrate that: compared with turbine only rotating in constant inflow, the instantaneous value of the axial loads coefficient, power coefficient, and yawing moment coefficient generate fluctuation, the fluctuation amplitudes of these three parameters have a positive correlation with the frequency and amplitude of the yawing motion and tip speed ratio; the frequency and amplitude of the yawing motion have little impact on yawing damping coefficient but this coefficient is positively proportioned to the rotational speed of the turbine. The results of this research can provide data to study the motion response of floating platform for floating tidal current turbine system and electric control design.

Keywords: Tidal current energy; Horizontal-axis turbine; Yawing; Hydrodynamic force; Damping coefficient

1. Introduction

Today, traditional fossil fuel energy is the main source of energy throughout the world; however, based on current mining trends, fossil fuel reserves will become depleted within the next few years. Therefore, an increasing number of countries have begun to develop clean and renewable energy resources [1], among which tidal current energy [2] is characterized by sustainability, high energy density, predictability and offshore location, and time changes like season and year have marginal effects on the energy output of this energy resource. Horizontal axis tidal turbine catches the attention of many scholars for experiencing less intense load changes in the flow field, stable power output, and smaller flow interference.

Tidal current turbines are the main area of development in the field of tidal current energy generation [3–5]. Turbines can be classified as either vertical axis turbines or horizontal axis turbines depending on the relative orientation of the main shaft and the flow direction. Many scholars focus on the horizontal axis turbine due to its load changing reposefully in the flow field, stable power output, and the smaller flow interference. Within tidal current energy station, the tidal current turbine [4,6–9] is an essential

* Corresponding author.

Part of the China–Pakistan Economic Corridor (CPEC) program.

component, the hydrodynamic performance directly determines the efficiency of the power station. Tidal current power station platforms support turbines, generators, other equipment, and personnel. In deep waters, floating moored systems [10] are the best platforms for tidal current turbines because of their advantages in terms of maintenance, removal, and installation. Therefore, the horizontal axis turbine with the floating platform is studied in this paper.

Scholars at home and abroad do a lot of researches on horizontal axis turbines. In 2013, Gaurier et al. [11] studied the effect of the interaction between wave and flow on the blade load of the tidal turbine. A 3 blades horizontal axis turbine is tested in a testing flume, and the radius of the turbine is 0.4 m. The effect of both current and wave-current interactions on measured strains is studied. These tests show that wave-current interactions can cause large additional loading amplitudes compared to currents alone, which must be considered in the fatigue analysis of these systems. In 2014, Galloway et al. [12] also carried out a similar model test on 3 blades horizontal turbine in towing tank, measuring the thrust torque and strain of the blade root of the turbine. The results show that: The maximum out-of-plane bending moment was found to be as much as 9.5 times the in-plane bending moment. A maximum loading range of 175% of the median out-of-plane bending moment and 100% of the median in-plane bending moment was observed for a turbine test case with zero rotors yawing, scaled wave height of 2 m, and an intrinsic wave period of 12.8 s. In 2014, Lust et al. [13] carried out the model test (wave and without wave) on 2 blades horizontal turbine in towing tank. The diameter of the model is 800 mm, and the immersing depth is 1.3 and 2.25 D. The resistance, torque, and rotational speed are tested. The test shows that the results in two immersing depths are similar and when the wave exists, the thrust and power experienced periodical change and the oscillation frequency is consistent with the wave frequency. Under different combinations of rotation speed and wave, the oscillation of test power and resistance are respectively 39% and as high as 79%. Similar hydrodynamic tests of the turbine were carried out by Barltrop et al. [14], Galloway et al. [15], and Luznik et al. [16]. Surface waves are generally adopted in the test, and the effects of surface waves on turbine performance have a lot to do with the immersing depth of the blade tip. Besides, the turbine usually is fixed on the trailer or sinks through the supporting component, with no movement. However, in practice, the floating platform suffers from wave movement, and the motion of the floating platform influences the horizontal axis turbine. The hydrodynamic performance of the horizontal axis turbine with the floating platform depends on the current velocity and the wave response motion of the tidal current power station (TCPS). It is important to study the relationship between the variation loads of the turbine and the movement of the floating platform.

Generally, the hydrodynamic loads of a turbine can be solved by computational fluid dynamic (CFD) or blade element momentum (BEM) methods [17–19]. In those methods, the loads are coupled with the motion of the turbine. In the 6 degrees of freedom (DOF) motion equations, the loads should be solved step-by-step. The calculations of the loads of turbines occupy significant CPU time and lower the efficiency of the numerical analysis. If loads of the turbine can be divided into added mass forces, damping forces, and exciting forces, and if the added mass forces, damping coefficients, and exciting forces can be previously determined, the solution of the 6 DOF motion equations of floating TCPS should be more efficient.

The hydrodynamic analysis of horizontal axis turbine with floating platform in wave-current field is very complicated, the hydrodynamic loads of the turbine depends on the current velocity, the rotating speed of the turbine, waves, and the motion of the platform. When the wave response motion is stable, the loads of the turbine may be expressed as an explicit function of the waves and the motion of the TCPS. So we simplify the hydrodynamic problems and put forward the following three assumptions: (1) the horizontal axis turbine is fixed on floating platform with main shaft, and floating platform has slightly simple harmonic motion with wave action; (2) the inflow velocity is a constant with no influence of waves, and the flux of the tidal speed is a small value; (3) the diameter of the turbine is smaller than wavelength, and the wave-making induced by turbine can be omitted. Based on the assumptions above, hydrodynamic problems of horizontal axis turbine in wave-current field can be simplified as problems of turbine with simple harmonic motion in a constant tidal current.

This paper is based on ANSYS CFX, using sliding mesh to analyze the hydrodynamic load in the unbounded and uniform stream when the horizontal axis turbine is forced to yawing. It also studies the influences of different yawing frequency, yawing amplitude, and tip speed ratio on turbine hydrodynamic load. The work has also followed the methods of Zhang et al. [20], which studied the effects of surge motion of the horizontal-axis tidal current turbine. Based on the numerical simulation results, a function was developed to fit the time history curves of the hydrodynamic loads to obtain the yawing damping coefficient according to the principle of least square method [21] and analyze the effects of yawing frequency, yawing amplitude and tip speed ratio in order to provide a reasonable hydrodynamic coefficient for further performance estimation of floating platform.

2. Basic theories

The inflow direction is defined as the forward direction of Z-axis, and Y-axis along the direction of gravity. The turbine moves around the axis parallel to the Y-axis. The yawing angular speed of the turbine is represented as ω_{sy} (unit: rad/s), the amplitude of yawing A_{sy} (unit: degree), the yaw center parallel the Y-axis and the distance between of Y-axis and roll center h (unit: m), the inflow speed U (unit: m/s), the diameter of the turbine D (unit: m), number of blades N, and rational speed of the turbine ω_T. Compared with the loads parallel to the inflow direction, loads perpendicular to it are marginal and the important factor considered here is the power coefficient. Therefore, all the simulations in this research neglected the loads perpendicular to the inflow direction and only study the axial load, the power coefficient, and Yawing moment.

Considering the convenience of analysis, the following dimensionless parameters are defined:

Tip speed ratio:

$$\lambda = \frac{\omega_T R}{U} \tag{1}$$

Dimensionless yawing angular speed of the turbine:

$$\bar{\omega}_{sy} = \frac{A_{sy}\omega_{sy}\cos(\omega_{sy}t)h_{sy}}{U} \tag{2}$$

Dimensionless yawing acceleration of the turbine:

$$\bar{a}_{sy} = -\frac{A_{sy}\omega_{sy}^2\sin\left(\omega_{sy}t\right)h_{sy}^2}{U^2} \tag{3}$$

Axial force coefficient of the turbine:

$$C_Z = \frac{F_Z}{0.5\rho U^2\pi R^2} \tag{4}$$

Yawing moment coefficient of the turbine:

$$C_{Tsy} = \frac{M_{sy}}{0.5\rho U^2\pi R^3} \tag{5}$$

Power coefficient:

$$C_P = \frac{M_Z\omega_T}{0.5\rho U^3\pi R^2} \tag{6}$$

where R (unit: m) is the radius of the turbine, F_Z (unit: N) is the axial force, M_{sy} (unit: Nm) is the yawing moment, M_Z (unit: Nm) is the axial torque, ρ (unit: kg/m^3) is the density of the inflow water.

C_{Tsy} can be expressed as:

$$C_{Tsy} = C_{Tsy}^F + n_{sy}\bar{\omega}_{sy} + m_{sy}\bar{a}_{sy} \tag{7}$$

where n_{sy} is the yawing damping coefficient:

$$n_{sy} = \frac{\delta C_{Tsy}}{\delta\bar{\omega}_{sy}} \tag{8}$$

and m_{sy} is the yawing added mass coefficient:

$$m_{sy} = \frac{\delta C_{Tsy}}{\delta\bar{a}_{sy}} \tag{9}$$

Considering the turbine with N blades, when the horizontal axis turbine rotates with a frequency of ω_T, overall hydrodynamics of the turbine oscillate with a frequency of $N\omega_T$, the hydrodynamic coefficients C_{Tsy}^F, n_{sy}, and m_{sy} in Eq. (6) can, respectively, be expressed by trigonometric series, as follows:

$$C_{Tsy}^F = C_{Tsy}^0 + \sum_{k=1}^{\infty} C_{Tsy}^k \sin\left(kN\theta(t) + \psi_{sy}^k\right) \tag{10}$$

$$n_{sy} = n_{sy}^0 + \sum_{k=1}^{\infty}\left[n_{sy}^k \sin\left(kN\theta(t) + \psi_{\omega sy}^k\right)\right] \tag{11}$$

$$m_{sy} = m_{sy}^0 + \sum_{k=1}^{\infty}\left[m_{sy}^k \sin\left(kN\theta(t) + \psi_{asy}^k\right)\right] \tag{12}$$

Thus, the hydrodynamic coefficients C_{Tsy} can be written in the form of series:

$$\begin{aligned} C_{Tsy} &= C_{Tsy}^F + n_{sy}\bar{\omega}_{sy} + m_{sy}\bar{a}_{sy} \\ &= C_{Tsy}^0 + \sum_{k=1}^{\infty} C_{Tsy}^k \sin\left(kN\theta(t) + \psi_{sy}^k\right) \\ &+ \left\{n_{sy}^0 + \sum_{k=1}^{\infty}\left[n_{sy}^k \sin\left(kN\theta(t) + \psi_{\omega sy}^k\right)\right]\right\}\bar{\omega}_{sy} \\ &+ \left\{m_{sy}^0 + \sum_{k=1}^{\infty}\left[m_{sy}^k \sin\left(kN\theta(t) + \psi_{asy}^k\right)\right]\right\}\bar{a}_{sy} \end{aligned} \tag{13}$$

The turbine hydrodynamic load coefficients C_{Tsy} in the time domain can be obtained by experiment or CFD simulation. If Eqs. (10)–(12) is truncated to finite items, the coefficients in Eq. (13) can be solved by the least-squares method. ANSYS CFX software uses the finite-volume method based on finite elements to provide the conservation characteristics of the finite-volume method combined with the accuracy of the finite-element method. Moreover, ANSYS CFX offers high accuracy in the simulation of rotating machinery because of its fully implicit coupled solver with multiple grids. Least-squares fits can be easily achieved through programming and have been widely applied for curve fitting. Therefore, the methodology used in this study relies on the least-squares method and CFD calculations with high simulation robustness.

Fig. 1 shows the flow diagram for the method used to study the hydrodynamic performance of a floating horizontal-axis tidal current turbine power station. CFD simulations and the least-squares method are used to obtain the added mass and damping coefficients for a turbine under yawing motion, which is the major research focus of this paper.

3. Numerical setting

3.1. Construction of computational domain

To monitor the stress state of a horizontal-axis turbine during yawing, ANSYS-CFX was used to simulate the operating conditions of the turbine in the presence of waves. The blade for calculation model is designed by Institute of Ocean Renewable Energy System (IORES) in Harbin Engineering University (HEU), China. The cross-section airfoil is S809, and the chord length and twist angle change with the radius, as shown in Table 1. Turbine diameter and blade number are 0.7 m and 2, respectively; the hub both ends are hemispherical, and the diameter is 0.1 D, as shown in Fig. 2a. Similar to Yang and Lawn [17], the whole computational domain is a square rectangular base, a square side length of 10 D, a rectangular length of 20 D. The distance between turbine rotation plane and the inlet

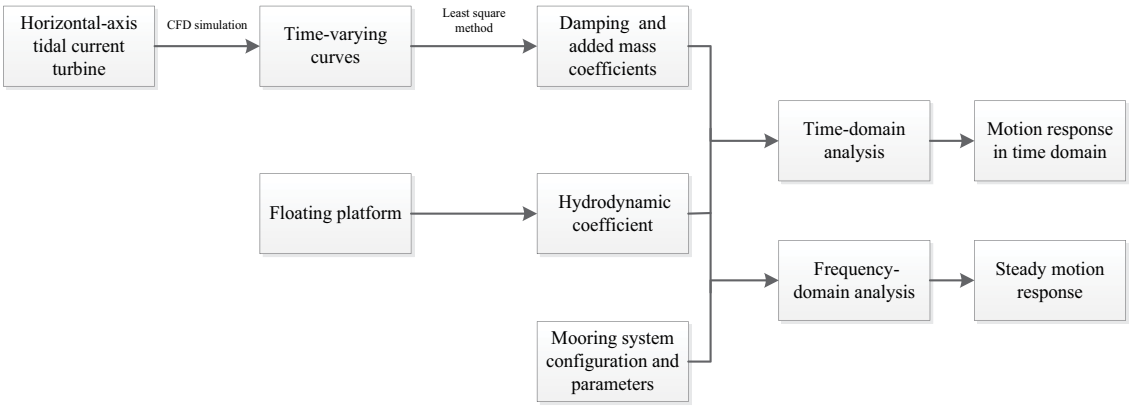

Fig. 1. Method of studying a floating horizontal-axis tidal current turbine power station.

Table 1
Turbine parameters

Radius (mm)	Chord (mm)	Pitch (°)
70	90.01	26.2
90	84.96	19.9
110	80.11	15.5
130	75.46	12.2
150	71.01	9.8
170	66.76	7.9
190	62.71	6.3
210	58.86	5.0
230	55.21	4.0
250	51.76	3.1
270	48.51	2.3
290	45.46	1.6
310	42.61	1.1
330	39.96	0.5
350	37.51	0.1

boundary is 5 D, as shown in Fig. 2b. During the numerical simulation in CFD, the rotation and yawing coupling motion of the turbine should be simulated simultaneously. In order to avoid the grid quality reduction in the process of calculation, the entire computational domain is divided into three parts, named stationary, yawing, and rotation domain. Rotation domain is within the yawing domain and yawing domain is within the stationary domain. The distance between the turbine rotating shaft and the center of yawing is 0.35 m. The calculation model is shown in Fig. 2.

3.2. Meshing

After the construction of the computational domain, the discrete method should be applied to the computational domain, namely, meshing. Meshing is a very important part of numerical simulation technology, but also more time-consuming. Grid quality directly affects the accuracy and efficiency of numerical calculation. In this paper, the mesh of the entire computational domain adopted the combination of structured grid and unstructured grid. Due to the complexity of blade shape, turbine rotation domain is adopted unstructured grid, but yawing domain and static domain are adopted structured grid. The minimum angle of the element is 20°, and the maximum mesh expansion factor is 1.2. Reference to the document [22], the height of the turbine surface mesh of the first layer is 0.0005 m, and the $y+$ ranges in 1–48. The total number of grids is 2.37 million, and the mesh grid model is shown in Fig. 3.

3.3. Boundary condition

Due to the turbine generate rotation and yawing coupling, sliding mesh is applied in rotation and yawing domain. Grid will not experience any translation in the process of motion, namely, the grid quality does not change in process of calculation, thus improving computing precision and computing speed. Specific settings: a yawing motion is given in the yawing section and rotation section, namely, the overall experiences simple harmonic rotating motion around the yawing center; rotation section is inside the yawing section and rotate around itself axis while yawing together with yawing section; grids in the stationary section are all stationary.

According to common calculation experience for horizontal axis turbines, the reference atmospheric pressure was established. The inlet boundary is set to velocity entry and given a uniform flow velocity U (1.5 m/s) and turbulence parameters. The outlet boundary uses the pressure outlet and given the average static relative pressure (0 Pa). The sides of the computational domain were defined as free-slip walls, and the turbine surfaces were defined as no-slip walls. The yawing and rotation domain were given yawing angular velocity, meanwhile the rotation domain was given grid position variation with time through subdomains. The rotation domain and yawing domain were connected by an interface, as were the yawing domain and the static domain. Besides, the SST model is adopted as the turbulent model and the transient solver is used. The time period during which the blade rotates 3° is adopted as the time step of the entire simulation, and the blades rotate around the Z-axis.

The turbulence model used in this paper is the SST model, which was proposed by Menter in 1994 [23]. The

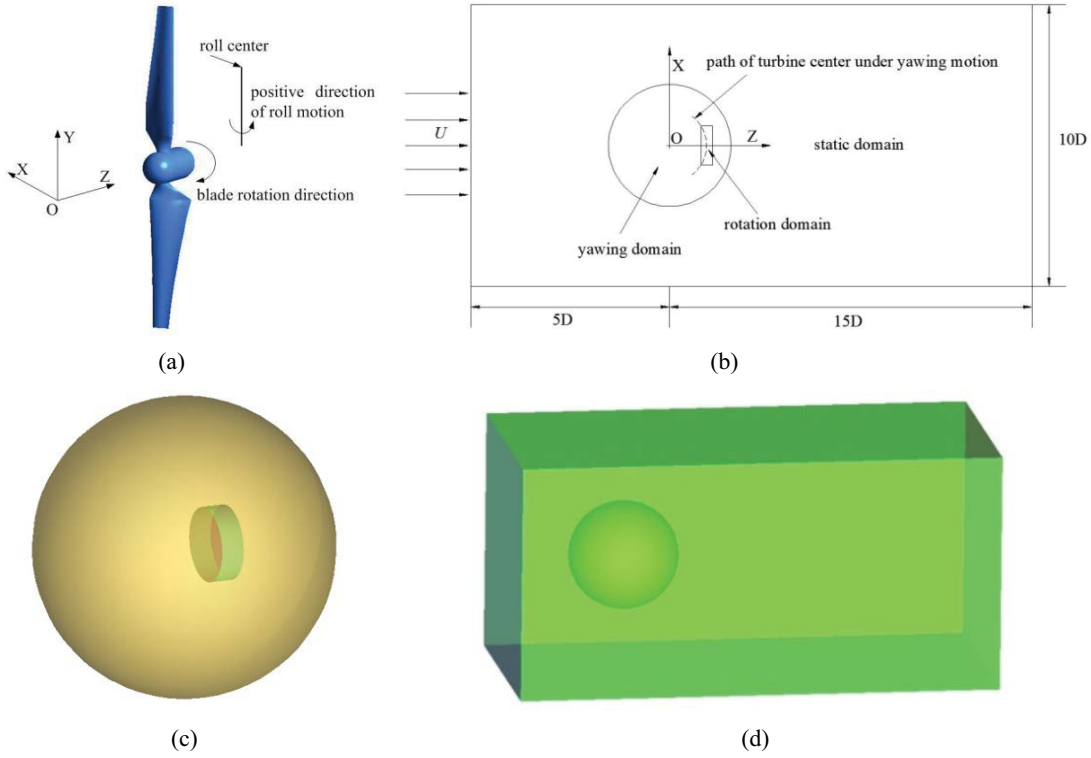

Fig. 2. Calculation model: (a) turbine, (b) schematic plan view, (c) yawing, and (d) static domain.

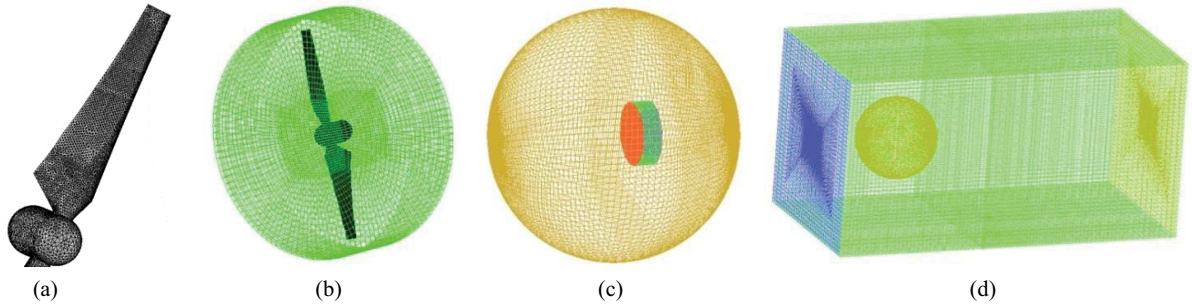

Fig. 3. Calculation model: (a) turbine, (b) rotation, (c) yawing, and (d) static domain.

SST model accurately captures the extreme pressure and velocity gradients in the vicinity of turbine blades. Many researchers have proven that the SST model is the most suitable model for calculations concerning turbines, including Wang et al. [24], Ponta and Dutt [25], and Shiono et al. [26].

4. Numerical analysis of blade loads

In order to validate the numerical simulation accuracy of horizontal axis turbine with grid model, the turbine is simulated in the uniform flow (velocity as 1.5 m/s and the drift angle is 0°) with a constant rotation motion under the same grid model in Fig. 4 and the calculated values of energy utilization ratio and axial load coefficient are compared with experimental values. The experimental values are tested in the towing tank of HEU, details of the experiment can be retrieved in this dissertation [27].

As shown in Fig. 4, the axial load increases, and the energy utilization ratio firstly increases and then decreases with the tip speed ratio (TSR) rises, the maximum output power coefficient (C_p) in experimental data is corresponding to the rotating speed 230 rpm of the turbine. The calculated and experimental values of these two parameters are in good agreement for most of the TSR values, except when the speed ratio is around 3. In fact, generally, the speed ratio is optimum when the energy utilization ratio is the maximum, and in the blade design process, the optimal speed ratio is related to the optimal angle of attack. When the speed ratio is larger than the optimal one, the blade section airfoil's angle of attack is smaller than the optimal one and the flow is not separated, which belongs to the problem of flows around with a small angle of attack. However, when the speed ratio is less than the optimal one, the blade section airfoil's angle of attack is larger than the optimal one

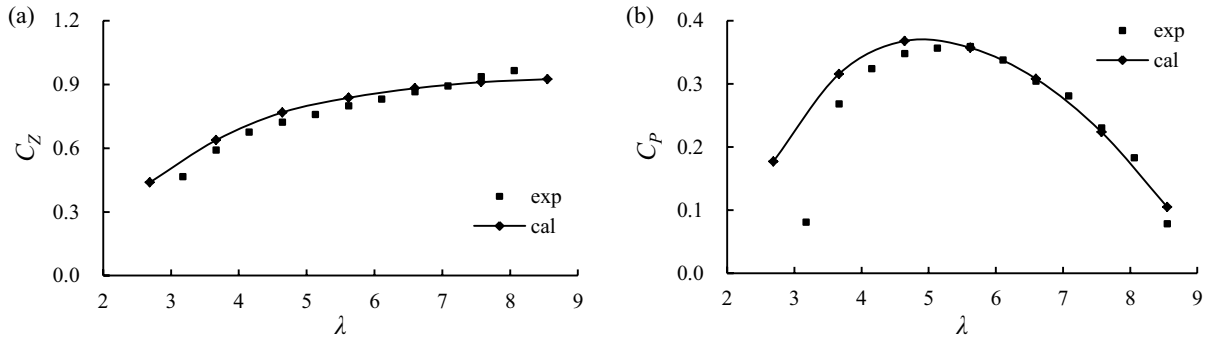

Fig. 4. Comparison between calculated and experimental values: (a) axial force and (b) power coefficient.

and the flow is separated. Especially when the speed ratios are further reduced, and even the stall phenomenon occurs so that there is a certain deviation between the calculation and the experimental results. Overall, the calculated and experimental results are in good agreement, which indicates that the ANSYS CFX simulation for horizontal-axis turbine hydrodynamics can achieve high precision. The type and quantity of mesh used in numerical verification are the same as the number used in simulated turbine occurs rotation and yaw coupled motion, so the impact from number and type of mesh on the numerical results can be ignored; during the process of yawing and rotational coupling motion simulation, the equivalent of a periodic velocity components increases in turbine rotation plane, but the maximum value (0.2094 m/s) is very small, which it doesn't change the nature of turbine operation. According to the above analysis, based on the same grid model, roll motion can be analyzed as follows and the numerical results are credible.

4.1. Effects of yawing frequency on loads of the turbine

In order to study the effect of different yawing frequencies on hydrodynamic performance of horizontal axis turbine, the yawing frequencies are selected in the common frequency range of wave, namely 0.4, 0.8, 1.2, 1.6, and 2.0 rad/s. The fixed rotational speed of the turbine is 230 rpm and the yawing amplitude is 15°. The initial position of the turbine is at the equilibrium position of yawing. The inlet velocity is 1.5 m/s. Fig. 5 shows axial force coefficient, power coefficient, and yawing moment coefficient of turbine changing curve with time under different yawing frequencies, wherein ω = 0 denotes no yawing motion.

According to Fig. 5, the axial force coefficient and power coefficient do not change with time when the turbine does not yaw. This is an important aspect of why a horizontal axis turbine is superior to a vertical axis turbine. When turbine yawing, the average value of axial

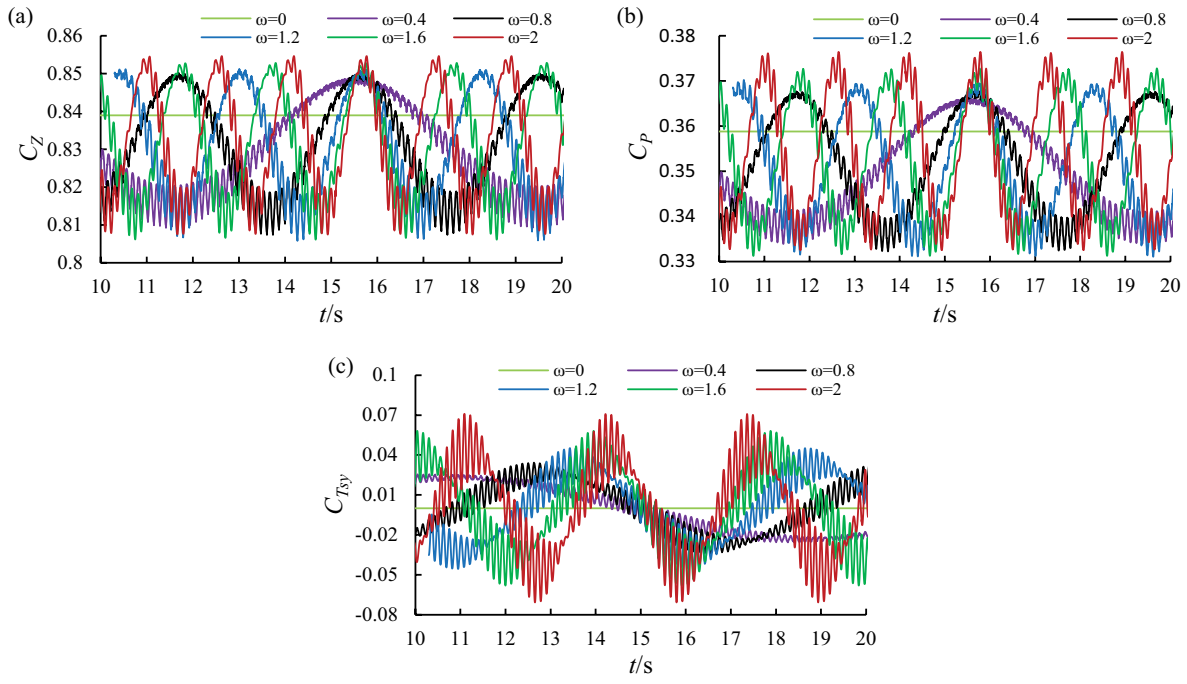

Fig. 5. Instantaneous value of different yawing frequencies (yawing amplitude 15°, rotational speed 230 rpm): (a) axial force, (b) power, and (c) yawing moment coefficient.

force coefficient and power coefficient is slightly smaller than that when no yawing; axial force coefficient, power coefficient, and yawing moment coefficient fluctuate obviously. The fluctuation frequency of axial force coefficient and power coefficient are consistent with double yawing frequency. The fluctuation frequency of yawing moment coefficient is consistent with yawing frequency, and the fluctuation amplitude of yawing moment coefficient slightly increases when the yawing frequency increases. When the turbine rotates, axial force coefficient, power coefficient, and yawing moment coefficient fluctuate slightly, and the frequency of slight fluctuate is consistent with double rotational frequency for 2 blades turbine. The axial force coefficient and power coefficient reach a maximum at the equilibrium position of yawing, and the maximum is bigger than when no yawing. The axial force coefficient and power coefficient reach minimum where the yawing reaches the maximum, and the minimum is basically same under different frequencies. The reason for this change is that: (1) the yawing motion produces a yaw angle between turbine rotational axle and inflow direction, and yaw angle change over time, but the maximum yaw angle is same (15°); (2) yawing motion makes the turbine produce velocity components changing over time in the rotating plane, and the bigger the yawing frequency, the greater the velocity changing range. The effect is equivalent to the periodic change of inflow velocity, thus leading to the fluctuation of the turbine load, which has negative impacts on the stability of power output and safety of structure of the turbine.

In order to reflect the effect of different yawing frequencies on average value of the power coefficient and axial force coefficient, this paper presents the trends of the average value of the power coefficient and axial force coefficient under different yawing frequencies. Fig. 6 shows that the power coefficient and axial force coefficient exhibits minimal variations with varying yawing frequencies at the tip speed ratio (λ = 5.62) because the changes in the fluid velocity distribution around the turbine are equivalent to the phenomenon in which the turbine is moving with a complicated velocity profile. Occasionally, the velocity distribution around the turbine under yawing motion is more complex than that under non-yawing motion.

4.2. Effects of yawing amplitude on loads of the turbine

In order to study the effects of yawing amplitude on loads of the turbine, three kinds of yawing amplitude (10°, 15°, and 20°) is calculated in this part. The initial position of turbine is at the equilibrium position of yawing. The inlet velocity is 1.5 m/s. Graphs in Fig. 7 show that axial force coefficient, power coefficient, and yawing moment coefficient under different yawing amplitudes change with time. From Fig. 7, it is clear that as the yawing amplitude increases, the fluctuation amplitudes of the instantaneous value of the three parameters rise, and the amplitude of maximal slight amplitude fluctuation rises; under different amplitudes, the maximum value of load fluctuation has little change, but the minimum value changes clearly. These are caused by the periodical change of relative velocity. The bigger the yawing amplitude, the greater the changing ranges of yaw angle, thus the greater fluctuation amplitudes of loads. The fluctuation of power coefficient increases the difficulty of power output, and the fluctuation of axial force coefficient is bad for the safety of structure of the turbine.

In order to reflect the effect of different yawing amplitude on average value of the power coefficient and axial force coefficient, Fig. 8 shows the trends of the average value of the power coefficient and axial force coefficient under different yawing amplitude. The average value of the power coefficient and axial force coefficient are slightly decreased with increasing in amplitude at the tip speed ratio (λ = 5.62) because the maximum of yawing angle will become great when the yawing amplitude is large.

4.3. Effects of tip speed ratio on loads of the turbine

Loads on the turbine should be stable if the yawing motion of the turbine is not taken into consideration. This section discusses changing rules of turbine load with different speed ratios under the same roll motion. The inlet velocity is 1.5 m/s. The initial position of turbine is at the equilibrium position of yawing. Five different rotational speeds (150, 190, 230, 270, and 310 rpm) are calculated, axial load coefficient, power coefficient, and yawing moment coefficient changing curves with time are shown in Fig. 9. From Fig. 9, the fluctuation amplitudes of the three

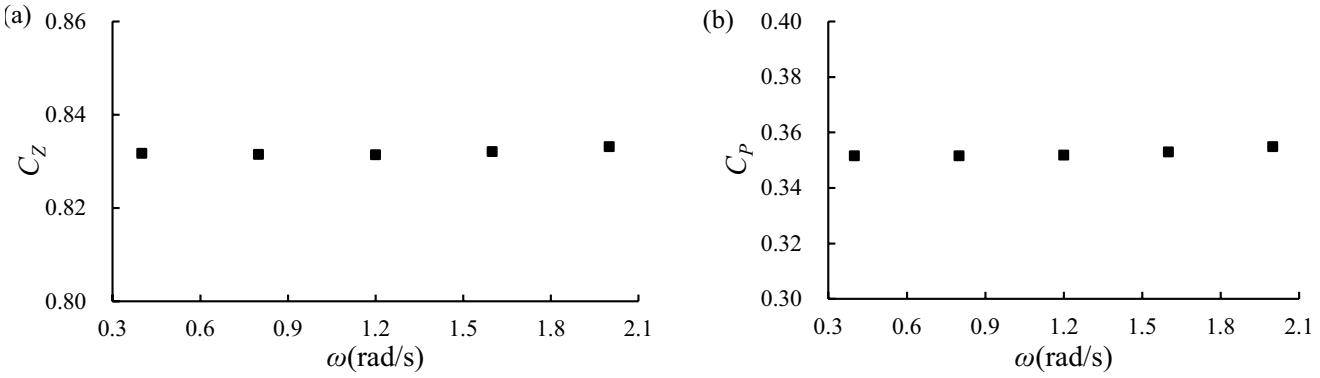

Fig. 6. Average value of different yawing frequencies (yawing amplitude 15°, rotational speed 230 rpm): (a) axial force and (b) power coefficient.

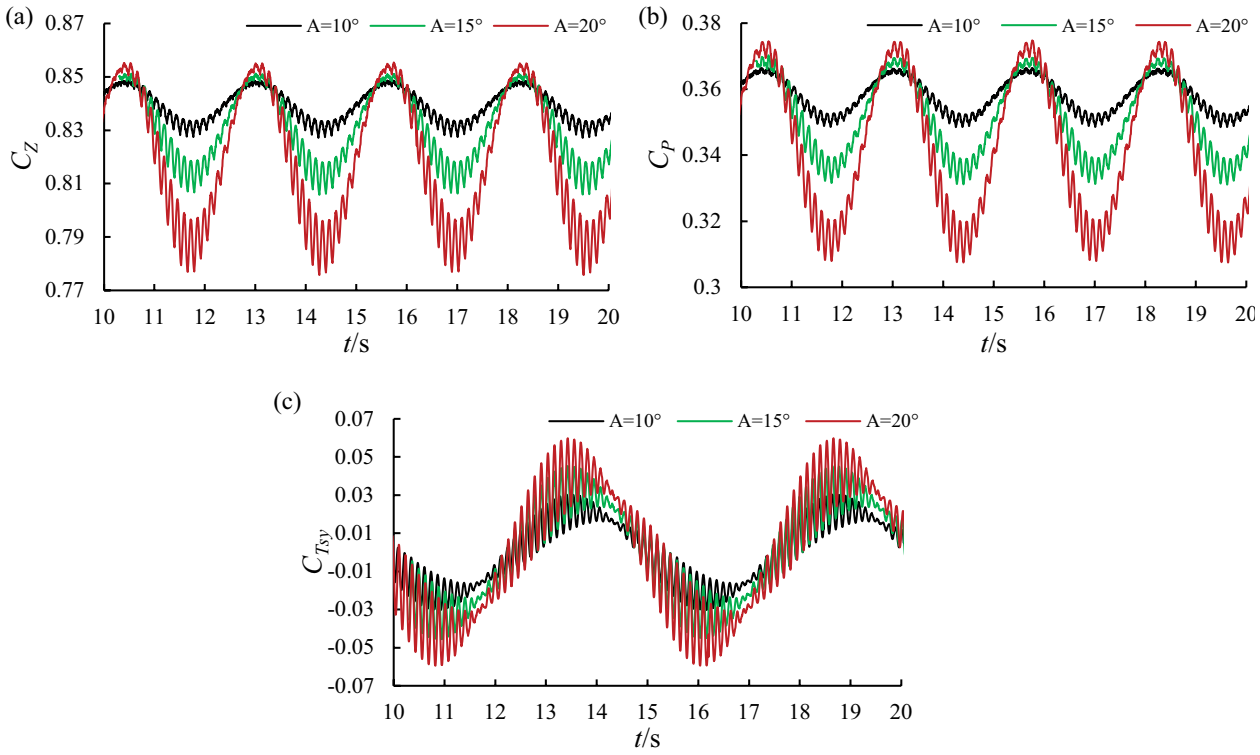

Fig. 7. Instantaneous values of different yawing amplitude (yawing frequency 1.2 rad/s, rotational speed 230 rpm): (a) axial force, (b) power, and (c) yawing moment coefficient.

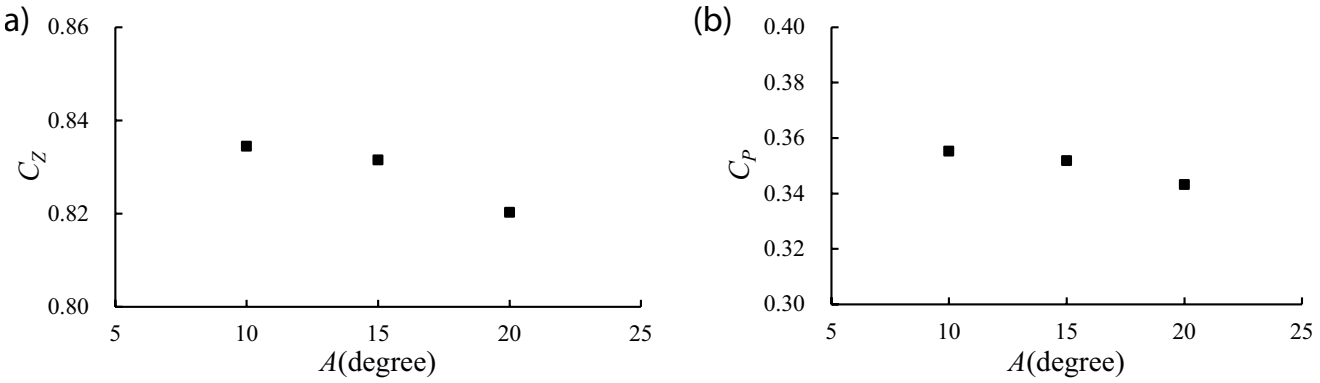

Fig. 8. Average value of different yawing amplitude (yawing frequency 1.2 rad/s, rotational speed 230 rpm): (a) axial force and (b) power coefficient.

parameters increases with the increases of turbine rotational speed; when position of turbine is at the maximum position of yawing motion, the fluctuation of turbine load based on the rotation frequency of turbine is obvious, and the amplitude of fluctuation increases with rotational speed increases. The reason is that when the yawing of turbine reaches the maximum, the yaw angle reaches the maximum (15°); the bigger the yaw angle, the greater the difference of the magnitude and direction of relative inflow when the blades are different azimuthal angles, resulting the obvious fluctuation of load.

Fig. 10 shows the trends of the average value of the power coefficient and axial force coefficient under different tip speed ratios. The average value of the power coefficient with yawing motion is smaller than that without yawing motion obviously, and not clearly in axial force coefficient. In most cases, the average value of the power coefficient represents the average annual electricity production. Therefore, the annual energy production of such a turbine under yawing motion will reduce some.

4.4. Analysis of flow field characteristics

In order to research the influence on the turbine trailing vortex by yawing movement, Fig. 11 shows the bird's eye view of equal vortex when the turbine is at the two different

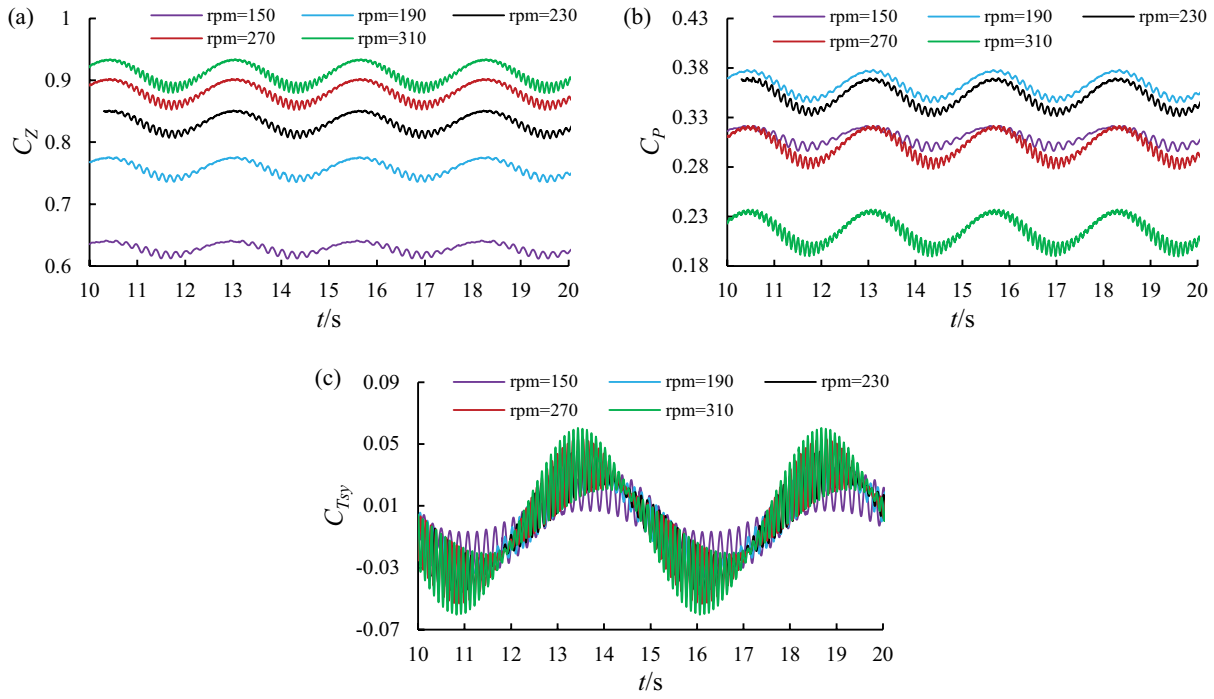

Fig. 9. Instantaneous values of different rotational speed (yawing frequency 1.2 rad/s, yawing amplitude 15°): (a) axial force, (b) power, and (c) yawing moment coefficient.

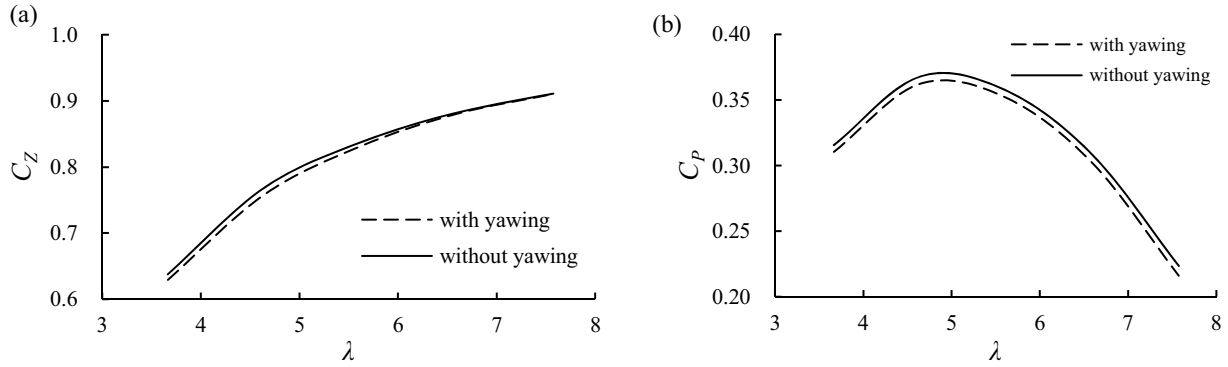

Fig. 10. Average value of different tip speed ratio (yawing frequency 1.2 rad/s, yawing amplitude 15°): (a) axial force and (b) power coefficient.

positions of yawing. In Fig. 11, the inflow speed is 1.5 m/s; vortex intensity is 6 s^{-1}. As shown in Fig. 9, in the process of turbine rotating, the trailing vortex near the water turbine is obvious spiral, and the trailing vortex sheds from the blade and root into the flow field, spreading gradually in the process of transmission with the vortex intensity abate and spiral trailing vortex gradually disappearing. From the comparison of the two figures, it can be found that the trailing vortex is basically symmetric, namely, when the blade is at the symmetric position of yawing, the trailing vortex is symmetric, thus resulting in the fluctuation frequency of axial force coefficient and power coefficient are consistent with double yawing frequency.

In order to research the influence on the turbine wake velocity by different yawing frequencies, the planar velocity contour under different yawing amplitudes is shown in Fig. 12. Contour shows the magnitude of the physical velocity, which reflects the distribution of the magnitude of the velocity on the planar. The plane is parallel to XOZ plane under the coordinate system as shown in Fig. 2 and cross the rotating axis and blades of the turbine. In Fig. 12, the position of the turbine is at the equilibrium position of yawing. The yawing will not occur when the amplitude is 0°, namely, the turbine rotates around a fixed axis in the uniform flow. As can be seen from Fig. 10, when the amplitude of yawing is 0, planar velocity distribution is basically symmetric, and the low-pressure area is obvious in the blade wake. When the turbine yaws, the planar velocity distribution is obviously different from that when no yawing and the low velocity area luffing. The

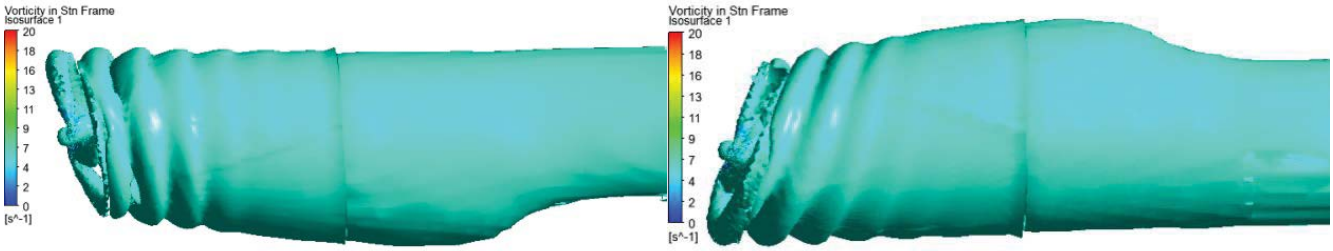

Fig. 11. Level of equal vortex in different position (rotational speed 230 rpm, yawing frequency 1.2 rad/s, and yawing amplitude 20°). The maximal position of (a) positive and (b) negative.

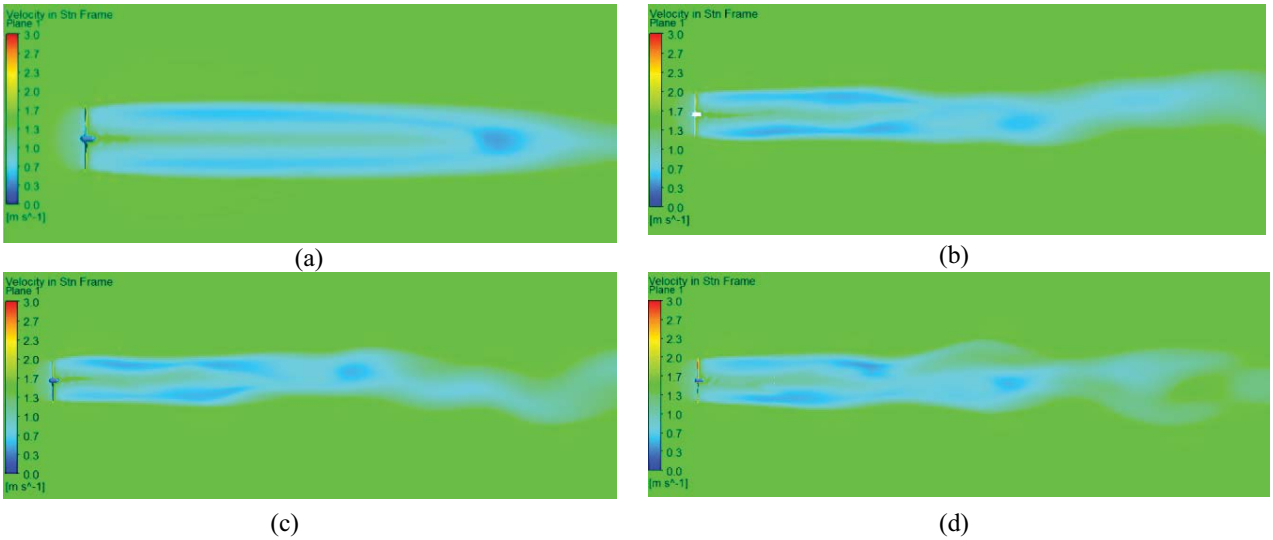

Fig. 12. Planar velocity contours (rotational speed 230 rpm, yawing frequency 1.2 rad/s). Yawing amplitude of (a) 0°, (b) 10°, (c) 15°, and (d) 20°.

greater the amplitude, the more obvious the luffing of the low velocity area, which increases the instability of blade wake, thus leading to the fluctuation of turbine load.

5. Fitting analysis of the damping coefficient

5.1. Effects of yawing frequency on damping coefficient

According to Eq. (12), the least square fitting method is applied on the time-varying yawing moment coefficient curves under different yawing frequencies to gain the hydrodynamic coefficients, as shown in Table 2. Table 1 only shows the constant terms and first-order terms of the expansion coefficients of C_{Tsy}.

As can be seen from Table 2, in the expansion coefficients of C_{Tsy}, the magnitudes of C_{Tsy} and C^1_{Tsy} are basically zero. With the increase of yawing frequency, the coefficients related with the damping coefficient are basically constant, namely, the damping coefficients of yawing have nothing to do with the yawing frequency, but the damping coefficients of yawing will experience periodical change with the change of blade azimuth angle. The added mass coefficient of m^0_{sy} and m^1_{sy} gradually decrease with the increase of yawing frequency. Yawing frequency affects the magnitude of yawing angular velocity and yawing angular acceleration, so when the rotational speed and yawing amplitude is constant, the fluctuation caused by yawing frequency depends on the magnitude of n^0_{sy} and m^0_{sy}, but the fluctuation caused by blade rotation depends on the magnitude of n^1_{sy} and m^1_{sy}.

5.2. Effects of yawing amplitude on damping coefficient

Table 3 shows the constant terms and first-order terms of the expansion coefficients of C_{Tsy} under different yawing amplitudes. As can be seen from Table 2, in the expansion coefficients of C_{Tsy}, with the increase of yawing amplitude, the magnitudes of C^0_{Tsy} and C^1_{Tsy} are zero; the coefficients related with the damping coefficient are basically constant, namely, the damping coefficients of yawing have nothing to do with the yawing amplitude; the coefficients related with the added mass coefficient are basically constant, namely, the added mass coefficients of yawing have nothing to do with the yawing amplitude. Yawing amplitude affects the magnitude of yawing angular velocity and yawing angular acceleration, so when the rotational speed and yawing frequency is constant, the fluctuation amplitude of C_{Tsy} varying with time depends on the magnitude of yawing amplitude.

5.3. Effects of tip speed ratio on damping coefficient

Table 4 shows coefficients for the constant terms and first-order terms of the expansion coefficients of C_{Tsy} under different rotational speeds.

As can be seen from Table 4, in the expansion coefficients of C_{Tsy}, with the increase of rotational speed, the magnitudes of C^0_{Tsy} and C^1_{Tsy} are zero; the absolute value of n^0_{sy} and n^1_{sy} related with the damping coefficient are gradually increase and the magnitude of $\psi^1_{\omega sy}$ is constant, namely, the damping coefficients increase with the rotational speed increase; the magnitude of m^0_{sy} gradually increase. So when the yawing amplitude and yawing frequency is constant, the fluctuation amplitude of C_{Tsy} caused by yawing motion depends on the magnitude n^0_{sy} and m^0_{sy}.

5.4. Verification of fitting formula

In order to verify the accuracy of the fitting method, coefficients in Tables 2–4 are put into the fitting formula and compared with the numerical solution from CFD, as shown in Fig. 13. 2-15-230-CFD and 2-15-230-EXP in Fig. 13 are, respectively, the numerical solution of CFD and the solution of fitting formula when yawing frequency, yawing amplitude, and rotational speed are, respectively, 2 rad/s, 15°, and 230 rpm. 1.2-15-310-CFD and 1.2-15-310-EXP in Fig. 13 are, respectively, the numerical solution of CFD and the solution of fitting formula when yawing frequency, yawing amplitude, and rotational speed are respectively1.2 rad/s, 15°, and 310 rpm. As can be seen from Fig. 13, the solution of the fitting formula is in good accordance with the numerical solution of CFD, which verifies the accuracy of the fitting method. Finally, based on the

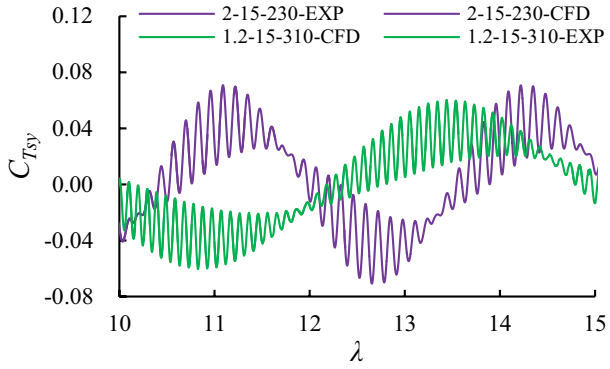

Fig. 13. Comparison between calculated and fitting values.

Table 2
C_{Tsy} expansion coefficient table (yawing amplitude 15°, rotational speed 230 rpm)

ω_{sy}	C^0_{Tsy}	C^1_{Tsy}	Ψ^1_{sy}	n^0_{sy}	n^1_{sy}	$\Psi^1_{\omega sy}$	m^0_{sy}	m^1_{sy}	Ψ^1_{asy}
0.4	0.000	0.0000	4.53	–0.331	0.2166	–123.86	9.577	0.7444	179.14
0.8	0.000	0.0000	34.76	–0.330	0.2170	–123.37	2.385	0.1823	–170.36
1.2	0.000	0.0000	–105.80	–0.331	0.2204	–122.48	1.054	0.0834	–155.82
1.6	0.000	0.0000	88.22	–0.333	0.2241	–122.34	0.592	0.0513	–151.24
2.0	0.000	0.0000	–74.51	–0.332	0.2278	–121.52	0.367	0.0382	–145.92

Table 3
C_{Tsy} expansion coefficient table (yawing frequency 1.2 rad/s, rotational speed 230 rpm)

A_{sy}	C^0_{Tsy}	C^1_{Tsy}	Ψ^1_{sy}	n^0_{sy}	n^1_{sy}	$\Psi^1_{\omega sy}$	m^0_{sy}	m^1_{sy}	Ψ^1_{asy}
10	0.000	0.0000	–16.14	–0.332	0.2204	–122.77	1.072	0.0860	–158.79
15	0.000	0.0000	–105.80	–0.331	0.2204	–122.48	1.054	0.0834	–155.82
20	0.000	0.0000	–6.41	–0.329	0.2181	–122.87	1.029	0.0839	–149.44

Table 4
C_{Tsy} expansion coefficient table (yawing frequency 1.2 rad/s, yawing amplitude 15°)

rpm	C^0_{Tsy}	C^1_{Tsy}	Ψ^1_{sy}	n^0_{sy}	n^1_{sy}	$\Psi^1_{\omega sy}$	m^0_{sy}	m^1_{sy}	Ψ^1_{asy}
110	0.000	0.0001	–175.56	–0.060	0.0894	–58.08	0.014	1.0792	155.96
150	0.000	0.0000	–33.20	–0.160	0.0997	–90.47	0.761	0.7149	170.86
190	0.000	0.0000	153.55	–0.282	0.1704	–123.55	0.979	0.2976	–153.96
230	0.000	0.0000	–105.80	–0.331	0.2204	–122.48	1.054	0.0834	–155.82
270	0.000	0.0000	74.23	–0.372	0.2666	–119.20	1.112	0.1154	45.93
310	0.000	0.0000	–23.23	–0.415	0.3098	–116.40	1.148	0.2235	25.76
350	0.000	0.0000	8.59	–0.457	0.3476	–113.47	1.156	0.2866	10.56

fitting formula and the coefficients in Tables 2–4, we can rapidly calculate the yawing moment coefficient within a certain range of yawing frequency and amplitude.

5.5. Application of turbine simulations

The above three tables show the expansion coefficients for yawing moment under different yawing frequencies and yawing amplitude and rotational speed. From these results, we can obtain a series of expansion coefficients for any yawing motion (frequencies 0.4–2.0 rad/s, amplitude 10°–20°, rotation speed 110–350 rpm) through interpolation. Then, these expansion coefficients can be applied to a floating turbine platform to simulate the yawing motion responses of the platform. Therefore, we can obtain the motion response under any yawing motion for a floating horizontal-axis tidal current turbine station, which will be a key focus of our future research.

We know that the hydrodynamic coefficients of the platform and mooring system are introduced to analyze the time- and frequency-domain motion responses from Fig. 2. Therefore, our future work will be to analyze the response of the entire floating turbine power station in the time and frequency domains.

6. Conclusions

A three-dimensional simulation by CFX is conducted concerning the hydrodynamic performance of a compulsorily-oscillated horizontal-axis turbine within a constant inflow environment. The least-square fitting is used to get the coefficients in the C_{Tsy} series. The study demonstrates that:

- Yawing motion of the turbine in a floating TCPS should be taken into consideration in the design stage, as it induces the fluctuation of axial force coefficient, power coefficient, and yawing moment coefficient, the fluctuation amplitudes of which have a positive correlation with yawing frequency, yawing amplitude and rotational speed (tip speed ratio) of the turbine, and these fluctuations have obvious negative impacts on the turbine's structural security, fatigue life, and the stability of electronic control system.
- The average of the axial force coefficient and power coefficient are slightly decreased by the yawing motion of turbine; therefore, the annual electricity output of the power station will be reduced.
- Instantaneous value of damping coefficient shows the periodical fluctuation in the process of rotation of turbine. The frequency of fluctuation is twice the rotational frequency of turbine (2 blades). The amplitude of fluctuation has nothing to do with the frequency and amplitude of yawing motion and have a positive correlation with rotational speed of turbine.
- The average of yawing damping coefficient is not relevant to the frequency and amplitude of yawing motion, but it has a positive correlation with rotational speed. This can provide effective support for the study of the motion response of the floating carrier.

Acknowledgments

This work was supported by the National Natural Science Foundation of China (no's. 51879125, 51709137, and U1706227), Natural Science Foundation of Jiangsu (BK20151327, BK20161103), Key University Science Research Project of Jiangsu (18KJA130001), Marine Equipment and Technology Institute of Jiangsu University of Science and Technology Funding Project (1174871801-17), Postgraduate Research and Practice Innovation Program of Jiangsu Province (KYCX18_2343, SJCX19_1187). Also, we thank associate professor Q.H. Sheng, who is working at Harbin Engineering University.

Symbols

U	—	Inflow velocity, m/s
ω_T	—	Turbine angular velocity, rad/s
D	—	Turbine diameter, m
N	—	Number of blades
R	—	Turbine radius, m
n	—	Rotation speed of turbine, r/min
F_Z	—	Axial force, N
M_Z	—	Axial torque, Nm
M_{sy}	—	Yawing moment, Nm
C_Z	—	Axial force coefficient
C_{Tsy}	—	Yawing moment coefficient
C_P	—	Power coefficient
ρ	—	Density of inflow water, kg/m^3
A_{sy}	—	Yawing amplitude, m
h	—	Distance between of Y axis and yaw center, m
ω_{sy}	—	Yawing angular speed, rad/s
$\bar{\omega}_{sy}$	—	Dimensionless yawing angular speed
$\bar{a}_{sy}$	—	Dimensionless yawing acceleration
n_{sy}	—	Yawing damping coefficient
m_{sy}	—	Yawing added mass coefficient
λ	—	Tip speed ratio

References

[1] S. Wang, P. Yuan, D. Li, Y. Jiao, An overview of ocean renewable energy in china, Renewable Sustainable Energy Rev., 15 (2011) 91–111.
[2] L. Zhang, X.Z. Li, J. Geng, X.W. Zhang, Tidal current energy update 2013, Adv. New Renewable Energy, 1 (2013) 53–68.
[3] Y. Ma, L. Zhang, L. Ma, Z. Chen, Development status and development trend of vertical axis turbine-type tidal current energy power generation device, Sci. Technol. Rev., 12 (2012) 71–75.
[4] W.M.J. Batten, A.S. Bahaj, A.F. Molland, J.R. Chaplin, The prediction of the hydrodynamic performance of marine current turbines, Renewable Energy, 33 (2008) 1085–1096.
[5] Y. Li, S.M. Çalişal, Numerical analysis of the characteristics of vertical axis tidal current turbines, Renewable Energy, 35 (2010) 435–442.
[6] Q.H. Sheng, D.Y. Zhao, L. Zhang, A design and numerical simulation of horizontal tidal turbine, J. Harbin Eng. Univ., 35 (2014) 389–394.
[7] J.H. Lee, S. Park, D.H. Kim, S.H. Rhee, M.-C. Kim, Computational methods for performance analysis of horizontal axis tidal stream turbines, Appl. Energy, 98 (2012) 512–523.
[8] A.S. Bahaj, A.F. Molland, J.R. Chaplin, W.M.J. Batten, Power and thrust measurements of marine current turbines under various hydrodynamic flow conditions in a cavitation tunnel and a towing tank, Renewable Energy, 32 (2007) 407–426.

[9] L.E. Myers, A.S. Bahaj, Experimental analysis of the flow field around horizontal axis tidal turbines by use of scale mesh disk rotor simulators, Ocean Eng., 37 (2010) 218–227.
[10] F. Jing, N. Mehmood, L. Zhang, G. Xiao, Optimal selection of floating platform for tidal current power station, Res. J. Appl. Sci. Eng. Technol., 6 (2013) 1116–1121.
[11] B. Gaurier, P. Davies, A. Deuff, G. Germain, Flume tank characterization of marine current turbine blade behaviour undercurrent and wave loading, Renewable Energy, 59 (2013) 1–12.
[12] P.W. Galloway, L.E. Myers, A.S. Bahaj, Quantifying wave and yawing effects on a scale tidal stream turbine, Renewable Energy, 63 (2014) 297–307.
[13] E.E. Lust, L. Luznik, K.A. Flack, J.M. Walker, M.C. Vab Benthem, The influence of surface gravity waves on marine current turbine performance, Int. J. Mar. Energy, 3 (2014) 27–40.
[14] N. Barltrop, K.S. Varyani, A. Grant, D. Clelland, X.P. Cham, Investigation into wave current interactions in marine current turbines, Proc. Inst. Mech. Eng., Part A: J. Power Energy, 42 (2007) 221–233.
[15] P.W. Galloway, L. Myers, A.S. Bahaj, Studies of Scale Turbine in Close Proximity to Waves, 3rd International Conference on Ocean Energy, Bilbao, 2010.
[16] L. Luznik, K.A. Flack, E.E. Lust Katharin Taylor, The effects of surface waves on the performance characteristics of a model tidal turbine, Renewable Energy, 58 (2013) 108–114.
[17] B. Yang, C. Lawn, Fluid dynamic performance of a vertical axis turbine for tidal currents, Renewable Energy, 36 (2011) 3355–3366.
[18] X.W. Zhang, S.Q. Wang, F. Wang, L. Zhang, Q.H. Sheng, The hydrodynamic characteristics of free variable pitch vertical axis tidal turbine, J. Hydrodyn., 24 (2012) 834–839.
[19] S. Khalid, L. Zhang, Three-dimensional numerical simulation of a vertical axis tidal turbine using the two-way fluid structure interaction approach, Appl. Phys. Eng., 14 (2013) 574–582.
[20] L. Zhang, S.Q. Wang, Q.H. Sheng, F.M. Jing, Y. Ma, The effects of surge motion of the floating platform on hydrodynamics performance of horizontal-axis tidal current turbine, Renewable Energy, 74 (2015) 796–802.
[21] L.Q. Zou, The least squares principle and simple application, Sci. Technol. Inf., 23 (2010) 282–238.
[22] S.Q. Wang, G. Xiao, L. Zhang, F. Jing, Supporting column influence analysis of horizontal axis tidal current turbine, J. Huazhong Univ. Sci. Technol., 42 (2014) 81–85.
[23] F.R. Menter, Two-equation eddy-viscosity turbulence models for engineering applications, AIAA J., 32 (1994) 1598–1605.
[24] S. Wang, D.B. Ingham, L. Ma, M. Pourkashanian, Z. Tao, Turbulence modeling of deep dynamic stall at relatively low Reynolds number, J. Fluids Struct., 33 (2012) 191–209.
[25] F. Ponta, G. Dutt, An improved vertical-axis water–current turbine incorporating a channelling device, Renewable Energy, 20 (2000) 223–241.
[26] M. Shiono, K. Suzuki, S. Kiho, Output characteristics of Darrieus water turbine with helical blades for tidal current generations, Proceedings of the 12th International Offshore and Polar Engineering Conference, Kitakyushu, Japan, 2002.
[27] S.Q. Wang, Chapter 2: Study on Hydrodynamic Characteristics of Horizontal Axis Tidal Current Turbine under Complicated Environment, Harbin Engineering University, Harbin, 2015.